

DISPLAY  
COPYImproved Rovibrational Constants and Frequency Tables for the  
Normal Laser Bands of  $^{12}\text{C}^{16}\text{O}_2$ F. RUSSELL PETERSEN, EARL C. BEATY, AND C. R. POLLOCK<sup>1</sup>*Time and Frequency Division, National Bureau of Standards, Boulder, Colorado 80303*

New frequency difference measurements between Doppler-free stabilized laser lines in the 9.4- and 10.4- $\mu\text{m}$  bands of  $^{12}\text{C}^{16}\text{O}_2$ , including high- $J$  and across-the-band-center measurements, have made significant improvements in the rovibrational constants. The absolute frequencies were referred to the methane stabilized 3.39- $\mu\text{m}$  He-Ne laser. Frequency tables generated from these constants have absolute uncertainties of less than two parts in  $10^{10}$  and are about a factor of 10 better than older tables. In addition, the laser lines  $P_1(50)$  in  $^{13}\text{C}^{16}\text{O}_2$  and  $R_{11}(26)$  in  $^{13}\text{C}^{18}\text{O}_2$ , which were used as reference lines in recent visible laser frequency measurements, were also measured to about the same accuracy.

## INTRODUCTION

The stabilized  $\text{CO}_2$  laser and its isotopic versions have become very important secondary frequency standards in the 10- $\mu\text{m}$  wavelength region of the spectrum. For example,  $\text{CO}_2$  has been used as a reference for the absolute frequency measurement of over 300 far infrared laser lines (1), many molecular absorption lines at 2.3  $\mu\text{m}$  (2), many laser lines between 5 and 6  $\mu\text{m}$  in CO (3), the 3.5- and 2.0- $\mu\text{m}$  laser lines in Xe (4), and the 3.39- and 1.15- $\mu\text{m}$  laser lines in Ne (5, 6). In two recent experiments extending laser frequency measurements into the visible at 576 and 633 nm (7, 8),  $\text{CO}_2$  was again used as a reference laser. Because the uncertainty in the visible measurements was desired to be of the order of  $1 \times 10^{-10}$  and the uncertainties in the  $\text{CO}_2$  frequencies were a few parts in  $10^9$  (9), an experiment was undertaken to improve these reference frequencies. This paper describes measurements which reduced uncertainties in the specific  $^{13}\text{C}^{16}\text{O}_2$  and  $^{13}\text{C}^{18}\text{O}_2$  reference lines for the visible frequency measurements. In the course of those measurements, the frequencies of a number of lines in the normal laser bands of  $^{12}\text{C}^{16}\text{O}_2$  were remeasured. Since this appeared to be an opportune time to redetermine the rovibrational constants for  $^{12}\text{C}^{16}\text{O}_2$  with higher accuracy, the measurements were extended to include frequency intervals across the band centers, lines near the band center, and high- $J$  lines. These data were combined with data from a previous (10, 11) measurement to produce improved rovibrational constants for the  $00^0_1-[10^0_0, 02^0_0]_1$  and  $00^0_1-[10^0_0, 02^0_0]_{11}$  bands of  $^{12}\text{C}^{16}\text{O}_2$ . Frequency tables generated from these constants are about a factor of 10 more accurate than older tables with an absolute uncertainty of less than two parts in  $10^{10}$ .

<sup>1</sup>NRC-NBS Postdoctoral Fellow, 1980-82. Present address: School of Electrical Engineering, Phillips Hall, Cornell University, Ithaca, N. Y. 14853.

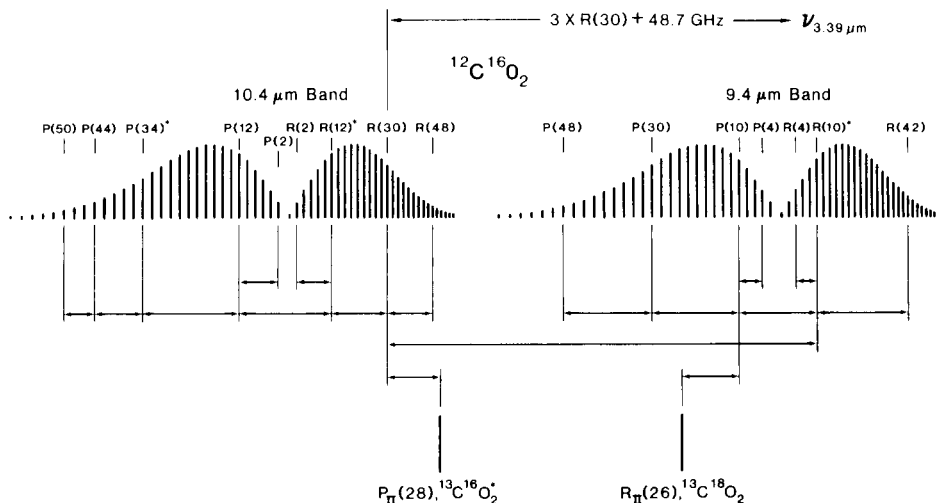


FIG. 1. Schematic showing the frequency interval measurements connecting the 9.4- and 10.4- $\mu\text{m}$  bands of  $^{12}\text{C}^{16}\text{O}_2$  and the isotopic lines  $P_{\text{II}}(28)$  in  $^{13}\text{C}^{16}\text{O}_2$  and  $R_{\text{II}}(26)$  in  $^{13}\text{C}^{18}\text{O}_2$  with the 3.39- $\mu\text{m}$   $\text{CH}_4$  reference. Lines denoted by an asterisk were used to connect  $P_1(50)$  in  $^{13}\text{C}^{16}\text{O}_2$  to the  $\text{CH}_4$  reference via the two schemes  $P_1(50) \cong 2R_1(12) - R_{\text{II}}(10)$  and  $P_1(50) \cong 2P_1(34) - P_{\text{II}}(28)$ ,  $^{13}\text{C}^{16}\text{O}_2$ .

#### EXPERIMENTAL DETAILS

The most accurately measured laser frequency standard is the 3.39- $\mu\text{m}$  He-Ne laser stabilized by the technique of saturated absorption on the  $F_2(2)$  component of the  $P(7)$  line in the  $\nu_3$  band of  $\text{CH}_4$ . We have taken the unweighted mean of the four most recently reported frequency measurements of the methane line (12-15), unresolved for hyperfine structure, which gives the value  $\nu_{3.39 \mu\text{m}} = 88\,376\,181.609$  MHz. A conservatively estimated uncertainty of  $\pm 9$  kHz ( $\Delta\nu/\nu = \pm 1 \times 10^{-10}$ ) was assigned to include each of the four measurements in the average.

The principal scheme employed in this experiment was to remeasure  $\text{CO}_2$  laser lines of interest with respect to the methane reference standard. Figure 1 shows how these measurements were accomplished. First, the difference between the third harmonic of  $R_1(30)^2$  in  $^{12}\text{C}^{16}\text{O}_2$  and  $\nu_{3.39}$  was remeasured to establish an absolute reference frequency at 10  $\mu\text{m}$ . The previously measured interband difference  $R_{\text{II}}(10) - R_1(30)$  was used to establish the reference frequency at 9  $\mu\text{m}$  (5). The doubled-ended arrows in Fig. 1 show the frequency intervals for each band which were measured in this experiment. The  $^{12}\text{C}^{16}\text{O}_2$  lasers oscillated on all lines in the intervals  $P_1(50)$  to  $P_1(2)$ ,  $R_1(2)$  to  $R_1(48)$ ,  $P_{\text{II}}(48)$  to  $P_{\text{II}}(4)$ , and  $R_{\text{II}}(4)$  to  $R_{\text{II}}(42)$ . As can be seen, large step measurements across the complete lasing bands, including measurements across the band centers, were taken.

For the visible frequency measurement at 576 nm (7),  $P_1(50)$  in  $^{13}\text{C}^{16}\text{O}_2$  was chosen as the laser reference line ( $\sim 1/20$  of the visible frequency). This line is too low in frequency for ready comparison with methane. Therefore, a frequency near  $P_1(50)$  was synthesized by a  $2\nu_1 - \nu_2$  scheme, where  $\nu_1$  and  $\nu_2$  were two  $\text{CO}_2$  laser lines whose

<sup>2</sup> On  $\text{CO}_2$  spectroscopic notation: Subscripts I and II refer to the  $00^0_1 - [10^0_0, 02^0_0]_{\text{I}}$  and  $00^0_1 - [10^0_0, 02^0_0]_{\text{II}}$  bands, respectively.

frequencies could be more easily compared with the methane frequency. Two different combinations,

$$P_I(50), {}^{13}\text{C}^{16}\text{O}_2 \cong 2R_{II}(12) - R_{II}(10) \quad (1)$$

and

$$P_I(50), {}^{13}\text{C}^{16}\text{O}_2 \cong 2P_I(34) - P_{II}(28), {}^{13}\text{C}^{16}\text{O}_2, \quad (2)$$

were used to check for closure in the measurements. The frequencies of the four lines involved in these synthesis schemes were measured by summing the appropriate intervals relative to  $\nu_{3.39\ \mu\text{m}}$  as shown in Fig. 1. In successive measurements, each line was associated with a specific laser. Since the day-to-day variation in the reproducibility of the frequency of a given laser was less than one part in  $10^{10}$ , the frequency shifts associated with a particular laser were not important in the sense that the lasers were used as transfer oscillators connecting  $P_I(50)$  with the methane frequency.

In the same spirit,  $R_{II}(26)$  in  ${}^{13}\text{C}^{18}\text{O}_2$  ( $\sim 1/4$  of the 2.39- $\mu\text{m}$  Ne frequency), which was used as a reference in the 633-nm visible frequency measurement (8), was measured relative to methane via  $P_{II}(10)$ ,  $R_{II}(10)$ , and  $R_I(30)$ .

With the exception of the  $P_I(50)$   ${}^{13}\text{C}^{16}\text{O}_2$  laser, all  $\text{CO}_2$  lasers were 1.25 m long. Mirror radii were either 4 or 10 m, and the reflectivities ranged from 80 to 90%. The efficiencies of the 150-grooves/mm gratings were about 95%. The lasers were stabilized with first derivative locking loops by the standing wave saturated fluorescence technique (16). Internal absorption cells at the grating end were filled to 5.3 Pa with  $\text{CO}_2$ .

The  $\text{CO}_2$  laser operating on  $P_I(50)$ ,  ${}^{13}\text{C}^{16}\text{O}_2$  was 2 m long with a 5-m radius, 95% reflectivity mirror, and a 150-grooves/mm grating for line selection. This laser was stabilized by the same technique except that an external absorption cell was used. The external beam parameters were adjusted to make the wave fronts planar at a flat Au coated mirror in the absorption cell. This mirror retroreflected the beam with about a 1-mrad angle of divergence to avoid feedback into the laser.

The 3.39- $\mu\text{m}$  portable methane stabilized laser used in the  $R_I(30)$  comparison utilized a 312-cm-radius output reflector with 12% transmittance at the end of a 28-cm, 2.5-mm bore, dc operated  ${}^3\text{He}$ - ${}^{20}\text{Ne}$  gain cell. A 27-cm absorber cell fitted with a Ba getter contained  $\text{CH}_4$  at a pressure of 1.6 Pa. The laser cavity was closed by a small plane mirror with 99% reflectance dithered at 15 kHz. A peak contrast of 1.2% led to a high signal-to-noise ratio in the third derivative locking loop. The frequency of this portable laser was compared with the JILA (Joint Institute for Laboratory Astrophysics) telescope laser (17) in an independent heterodyne experiment (18). At the chosen operating point (220  $\mu\text{W}$  emitted power and a modulation of 700 kHz peak-to-peak), the portable laser frequency was  $3.8 \pm 0.1$  kHz higher than the JILA telescope laser frequency, which was previously shown via ultrahigh resolution experiments to lock  $1.7 \pm 0.2$  kHz higher than the frequency of the central  $F = 7 \rightarrow 6$  hyperfine component in the  $\text{CH}_4$   $P(7)$   $F_2(2)$  line spectrum. The JILA telescope laser was assumed to operate within one part in  $10^{10}$  at 88 376 181.609 MHz or at the four measurement average taken for the methane stabilized laser frequency (19).<sup>3</sup>

<sup>3</sup> For a discussion of perturbations on the methane stabilized laser frequency, see J. L. Hall, "Sub-Doppler Spectroscopy, Methane Hyperfine Spectroscopy, and the Ultimate Resolution Limits," Colloques Internationaux du CNRS, No. 217, Méthodes de Spectroscopie sans Largeur Doppler de Niveaux Excités de Systèmes Moléculaires Simples, pp. 105-125, Centre National De La Recherche Scientifique, Paris, 1974.

Mixing and harmonic generation were done in a W-Ni point contact diode. The laser difference frequencies were synthesized by harmonics (up to 10) of klystrons at 8–12 and/or 59–65 GHz. Beat frequencies were usually signal averaged for 2 to 3 min along with marker frequencies for calibration. The relative phase and amplitude of the dither voltage modulating the frequencies of the two lasers were adjusted to minimize the width of the beat signal, which typically was about 50 kHz. Normally, about 10 of these signal averaged spectra were used for a given laser frequency difference determination. In some cases, a rf oscillator was phase-locked to the beat signal, and the frequency of the oscillator was counted.

## ANALYSIS OF THE RESULTS

Table I summarizes the results of the  $^{12}\text{C}^{16}\text{O}_2$  laser line difference frequency measurements. The most surprising results were those from measurements across the band centers, i.e.,  $R_{\text{I}}(12)-P_{\text{I}}(12)$  and  $R_{\text{II}}(10)-P_{\text{II}}(10)$ . These measured differences were

TABLE I

Summary of the New Experimental Data Used for Improving the Rovibrational Constants of  $^{12}\text{C}^{16}\text{O}_2$   
(The estimated experimental uncertainty in each difference frequency was about 3 kHz)

$^{12}\text{C}^{16}\text{O}_2$ $00^0_1-[10^0_0,02^0_0]_{\text{I}}$ Band (10.4 $\mu\text{m}$ )		
Laser Line Combination	Diff. Freq. (MHz)	Obs.-Calc. (MHz)
P(44) - P(50)	192 162.1695	0.0005
P(34) - P(44)	304 958.2085	0.0007
P(12) - P(34)	605 305.8709	0.0014
P( 2) - P(12)	245 814.2717	0.0037
R(12) - P(12)	580 247.7308	-0.0039
R(12) - R( 2)	218 371.9595	0.0033
R(30) - R(12)	346 208.9282	0.0009
R(34) - R(32)	33 905.8143	-0.0017
R(36) - R(34)	33 129.6499	0.0001
R(48) - R(30)	283 911.4428	0.0001

$^{12}\text{C}^{16}\text{O}_2$ $00^0_1-[10^0_0,02^0_0]_{\text{II}}$ Band (9.4 $\mu\text{m}$ )		
Laser Line Combination	Diff. Freq. (MHz)	Obs.-Calc. (MHz)
P(30) - P(48)	555 617.8600	-0.0001
P(10) - P(30)	545 351.1997	-0.0008
P( 4) - P(10)	148 265.2900	0.0013
R(10) - P(10)	487 423.5072	0.0013
R(10) - R( 4)	130 249.5076	-0.0006
R(42) - R(10)	573 995.5468	-0.0009

10 to 20 kHz larger than the values predicted with our previous constants (11), but still within the estimated experimental error.

Table II gives the results of the  $3.39 \mu\text{m}-R_1(30)$  comparison, the  $^{13}\text{C}^{16}\text{O}_2$  and  $^{13}\text{C}^{18}\text{O}_2$  data pertinent to the 576- and 633-nm visible frequency measurements, and the  $^{12}\text{C}^{16}\text{O}_2$  interband difference used in the analysis. The interband difference frequency was not measured in this experiment, and the value in Table II is taken from Ref. (5). That experiment, however, utilized  $\text{CO}_2$  lasers nearly identical to those used here, and the experimental uncertainty was comparable to the uncertainties in this experiment.

#### *New Rovibrational Constants for $^{12}\text{C}^{16}\text{O}_2$*

The experimental data in Table I were combined with those of Ref. (10) and used to obtain new rovibrational constants for  $^{12}\text{C}^{16}\text{O}_2$ . Expressions for the measured frequency differences were derived from the truncated power series expansion

$$T(v, J) = G(v) + B_v J(J+1) - D_v J^2(J+1)^2 + H_v J^3(J+1)^3 + L_v J^4(J+1)^4, \quad (3)$$

which was assumed to represent the energy of each rovibrational state. Values of the expansion coefficients were found which yielded the least mean squares error between the calculated and measured values. The least squares analysis was done with a thoroughly tested computer library routine which was derived from the widely distributed OMNITAB (20). The analysis included some elementary tests which indicated that the residuals were close to a Gaussian distribution and were not significantly

TABLE II

Summary of the  $\nu_{3.39 \mu\text{m}}-^{12}\text{C}^{16}\text{O}_2$  Comparison and the Measurements of the  $^{13}\text{C}^{16}\text{O}_2$  and  $^{13}\text{C}^{18}\text{O}_2$  Laser Lines Used in the Visible Laser Frequency Measurements

Laser Line Combination	Diff. Freq. (MHz)	Uncertainty (MHz)
$\nu_{3.39 \mu\text{m}}^a - R_1(30)$	48 731.6538	0.0024
$R_{11}(10) - R_1(30)$	2 691 783.5760 <sup>b</sup>	0.0020
$P_{11}(28), ^{13}\text{C}^{16}\text{O}_2 - R_1(30)$	328 184.8403	0.0021
$P_{11}(10) - R_{11}(26), ^{13}\text{C}^{18}\text{O}_2$	359 806.9768	0.0021
$[2R_1(12) - R_{11}(10)] - P_1(50), ^{13}\text{C}^{16}\text{O}_2$	22 941.9100	0.0037
$[2P_1(34) - P_{11}(28), ^{13}\text{C}^{16}\text{O}_2] - P_1(50), ^{13}\text{C}^{16}\text{O}_2$	15 433.4420	0.0037

(a) The frequency of the portable  $3.39 \mu\text{m}$  reference laser used in this experiment was blue-shifted from the JILA telescope laser by 3.8 (1) kHz. The JILA telescope laser was assumed to oscillate at 88 376 181.609(9) MHz, the mean of the four most recent measurements. Thus, the frequency of our reference laser was taken to be 88 376 181.613(9) MHz.

(b) Not measured in this experiment. Value taken from Ref. (5).

correlated with important variables of the problem. This analysis led to our acceptance of the hypothesis that the laser frequencies were subject to fluctuations caused by some internal process and that these fluctuations were the dominant cause of the inability to exactly represent the data with Eq. (3). The laser frequency noise implied by this analysis is approximately the same as that found in Ref. (11) and is also approximately what we would predict from estimates of the experimental uncertainties in each measurement.

The input data were weighted equally since the experimental uncertainties were all of comparable magnitude. The initial analysis with nine constants ( $B_v$ ,  $D_v$ ,  $H_v$ ) resulted in a distribution of residuals which departed significantly from a normal distribution. Consequently, the  $L_v$  terms (12 constants) were added. In this fit, the estimated uncertainty for  $L_{00^0_1}$  was about 22 times its magnitude while the uncertainties for  $L_I$  and  $L_{II}$  were comparable to their magnitudes. Therefore,  $L_{00^0_1}$  was set equal to zero, and 11 constants were used in the final fit. This resulted in no change in the remaining 11 constants but a significant reduction in the uncertainties of all of the constants. The standard deviation of the residuals was 2.5 kHz with 59  $df$ , and their distribution appeared to be normal. Table III lists the constants with their estimated standard errors from this final fit. Since linear combinations of the constants are used for estimation of line frequencies and in turn linear combinations of the line frequencies are often used for frequency synthesis purposes, the variance-covariance matrix is given in Table IV to enable calculation of estimated errors.

Table V lists the line frequencies for both the  $00^0_1-[10^0_0, 02^0_0]_I$  and  $00^0_1-[10^0_0, 02^0_0]_{II}$  bands and their estimated standard errors. Errors were propagated from reference lines  $R_I(30)$  and  $R_{II}(10)$ . The frequency of  $R_I(30)$  was adjusted upward by 4.7 kHz as a result of its measurement relative to the 3.39- $\mu\text{m}$  methane line (see Table II).

TABLE III

Rovibrational Constants for the  $00^0_1-[10^0_0, 02^0_0]_I$  and  $00^0_1-[10^0_0, 02^0_0]_{II}$  Bands of  $^{12}\text{C}^{16}\text{O}_2$  (Stated uncertainties in the constants are 1- $\sigma$  estimates. The 95% confidence interval estimate is obtained by multiplying the 1- $\sigma$  uncertainty by 2.0)

Constant	(MHz)
$B_{00^0_1}$	11 606.206 8792(391)
$D_{00^0_1}$	$3.987\,9498(279) \times 10^{-3}$
$H_{00^0_1}$	$4.1372(638) \times 10^{-10}$
$B_I$	11 697.569 3665(410)
$D_I$	$3.445\,8009(336) \times 10^{-3}$
$H_I$	$5.5687(133) \times 10^{-9}$
$L_I$	$1.839(214) \times 10^{-14}$
$B_{II}$	11 706.364 5771(428)
$D_{II}$	$4.711\,4318(416) \times 10^{-3}$
$H_{II}$	$7.0361(253) \times 10^{-9}$
$L_{II}$	$-4.377(585) \times 10^{-14}$

TABLE IV  
Variance-Covariance Matrix (in MHz<sup>2</sup>) for the Constants Given in Table III

	$B_{00}^0$	$B_I$	$B_{II}$	$D_{00}^0$	$D_I$	$D_{II}$	$H_{00}^0$	$H_I$	$H_{II}$	$L_I$	$L_{II}$
$B_{00}^0$	1.52627 $\times 10^{-9}$										
$B_I$	1.52103 $\times 10^{-9}$	1.68103 $\times 10^{-9}$									
$B_{II}$	1.50483 $\times 10^{-9}$	1.50294 $\times 10^{-9}$	1.83189 $\times 10^{-9}$								
$D_{00}^0$	7.82895 $\times 10^{-13}$	7.50321 $\times 10^{-13}$	7.27520 $\times 10^{-13}$	7.76773 $\times 10^{-16}$							
$D_I$	7.90861 $\times 10^{-13}$	1.01347 $\times 10^{-12}$	7.40995 $\times 10^{-13}$	7.44606 $\times 10^{-16}$	1.12981 $\times 10^{-15}$						
$D_{II}$	7.34133 $\times 10^{-13}$	7.16363 $\times 10^{-13}$	1.33913 $\times 10^{-12}$	5.58047 $\times 10^{-16}$	5.48532 $\times 10^{-16}$	1.73306 $\times 10^{-15}$					
$H_{00}^0$	1.48800 $\times 10^{-16}$	1.40490 $\times 10^{-16}$	1.37888 $\times 10^{-16}$	1.71892 $\times 10^{-19}$	1.64423 $\times 10^{-19}$	1.25592 $\times 10^{-19}$	4.06885 $\times 10^{-23}$				
$H_I$	1.68809 $\times 10^{-16}$	2.96023 $\times 10^{-16}$	1.60125 $\times 10^{-16}$	1.77786 $\times 10^{-19}$	4.00467 $\times 10^{-19}$	1.39360 $\times 10^{-19}$	4.30031 $\times 10^{-23}$	1.76892 $\times 10^{-22}$			
$H_{II}$	1.05683 $\times 10^{-16}$	1.11216 $\times 10^{-16}$	5.15153 $\times 10^{-16}$	-3.18563 $\times 10^{-20}$	-1.79212 $\times 10^{-20}$	8.76477 $\times 10^{-19}$	-2.18756 $\times 10^{-24}$	7.77049 $\times 10^{-24}$	6.40930 $\times 10^{-22}$		
$L_I$	-6.57754 $\times 10^{-21}$	-2.99924 $\times 10^{-20}$	-6.77653 $\times 10^{-21}$	-5.62217 $\times 10^{-24}$	-4.65714 $\times 10^{-23}$	-6.00195 $\times 10^{-24}$	-1.62714 $\times 10^{-27}$	-2.57912 $\times 10^{-26}$	-2.05787 $\times 10^{-27}$	4.56466 $\times 10^{-30}$	
$L_{II}$	1.10529 $\times 10^{-20}$	7.57570 $\times 10^{-21}$	-7.43352 $\times 10^{-20}$	5.15121 $\times 10^{-23}$	4.60186 $\times 10^{-23}$	-1.52785 $\times 10^{-22}$	1.06668 $\times 10^{-26}$	8.60224 $\times 10^{-27}$	-1.41011 $\times 10^{-25}$	1.46485 $\times 10^{-31}$	3.42683 $\times 10^{-29}$

TABLE V

Calculated Frequencies for the  $00^0_1$ - $[10^0_0, 02^0_0]_1$  and  $00^0_1$ - $[10^0_0, 02^0_0]_{b_{11}}$  Bands of  $^{12}\text{C}^{16}\text{O}_2$  with Estimated  $1-\sigma$  Relative and Absolute Uncertainties

Line	10.4 $\mu\text{m}$ Band		Line	9.4 $\mu\text{m}$ Band	
	Frequency (MHz)	Uncertainty Rel. (MHz) Abs. (MHz)		Frequency (MHz)	Uncertainty Rel. (MHz) Abs. (MHz)
P(60)	27077607.5028	0.0489 0.0490	P(60)	30143456.4867	0.2033 0.2033
P(58)	27146404.4486	0.0299 0.0300	P(58)	30212223.9629	0.1302 0.1303
P(56)	27214396.1696	0.0174 0.0177	P(56)	30280322.2857	0.0793 0.0794
P(54)	27281588.8619	0.0098 0.0103	P(54)	30347743.8416	0.0451 0.0452
P(52)	27347988.4136	0.0060 0.0068	P(52)	30414481.1847	0.0230 0.0233
P(50)	27413600.4115	0.0047 0.0056	P(50)	30480527.0438	0.0098 0.0104
P(48)	27478430.1485	0.0044 0.0054	P(48)	30545874.3292	0.0037 0.0052
P(46)	27542482.6301	0.0042 0.0052	P(46)	30610516.1388	0.0040 0.0054
P(44)	27605762.5805	0.0040 0.0051	P(44)	30674445.7651	0.0048 0.0060
P(42)	27668274.4492	0.0038 0.0049	P(42)	30737656.7010	0.0047 0.0060
P(40)	27730022.4165	0.0037 0.0048	P(40)	30800142.6463	0.0042 0.0056
P(38)	27791010.3990	0.0035 0.0047	P(38)	30861897.5132	0.0036 0.0051
P(36)	27851242.0547	0.0034 0.0046	P(36)	30922915.4319	0.0032 0.0049
P(34)	27910720.7883	0.0033 0.0046	P(34)	30983190.7566	0.0029 0.0047
P(32)	27969449.7555	0.0033 0.0045	P(32)	31042718.0701	0.0028 0.0046
P(30)	28027431.8676	0.0032 0.0045	P(30)	31101492.1893	0.0027 0.0046
P(28)	28084669.7958	0.0032 0.0044	P(28)	31159508.1695	0.0027 0.0046
P(26)	28141165.9746	0.0032 0.0044	P(26)	31216761.3094	0.0026 0.0045
P(24)	28196922.6060	0.0031 0.0044	P(24)	31273247.1550	0.0026 0.0045
P(22)	28251941.6621	0.0031 0.0044	P(22)	31328961.5037	0.0026 0.0045
P(20)	28306224.8891	0.0031 0.0044	P(20)	31383900.4084	0.0025 0.0045
P(18)	28359773.8096	0.0030 0.0043	P(18)	31438060.1802	0.0024 0.0044
P(16)	28412589.7252	0.0029 0.0042	P(16)	31491437.3923	0.0022 0.0043
P(14)	28464673.7190	0.0028 0.0042	P(14)	31544028.8828	0.0019 0.0042
P(12)	28516026.6577	0.0027 0.0041	P(12)	31595831.7569	0.0016 0.0040
P(10)	28566649.1936	0.0027 0.0041	P(10)	31646843.3898	0.0015 0.0040
P(8)	28616541.7658	0.0028 0.0042	P(8)	31697061.4282	0.0014 0.0040
P(6)	28665704.6019	0.0028 0.0042	P(6)	31746483.7927	0.0015 0.0040
P(4)	28714137.7193	0.0029 0.0042	P(4)	31795108.6785	0.0017 0.0041
P(2)	28761840.9257	0.0029 0.0043	P(2)	31842934.5572	0.0018 0.0041
V(0)	28808813.8201	0.0029 0.0043	V(0)	31889960.1772	0.0018 0.0041
R(0)	28832026.2179	0.0029 0.0043	R(0)	31913172.5751	0.0018 0.0041
R(2)	28877902.4362	0.0028 0.0042	R(2)	31958996.0677	0.0016 0.0040
R(4)	28923046.4283	0.0027 0.0041	R(4)	32004017.3875	0.0014 0.0039
R(6)	28967457.0638	0.0026 0.0040	R(6)	32048236.2545	0.0010 0.0038
R(8)	29011133.0037	0.0024 0.0039	R(8)	32091652.6662	0.0005 0.0037
R(10)	29054072.6995	0.0022 0.0038	R(10)	32134266.8957	0.0000 0.0037
R(12)	29096274.3924	0.0021 0.0038	R(12)	32176079.4916	0.0005 0.0037
R(14)	29137736.1122	0.0020 0.0037	R(14)	32217091.2759	0.0010 0.0038
R(16)	29178455.6756	0.0019 0.0037	R(16)	32257303.3427	0.0014 0.0040
R(18)	29218430.6852	0.0019 0.0036	R(18)	32296717.0558	0.0017 0.0041
R(20)	29257658.5273	0.0017 0.0036	R(20)	32335334.0465	0.0020 0.0042
R(22)	29296136.3697	0.0015 0.0035	R(22)	32373156.2114	0.0023 0.0043
R(24)	29333861.1596	0.0013 0.0033	R(24)	32410185.7086	0.0025 0.0045
R(26)	29370829.6209	0.0009 0.0032	R(26)	32446424.9556	0.0027 0.0046
R(28)	29407038.2514	0.0005 0.0031	R(28)	32481876.6251	0.0030 0.0048
R(30)	29442483.3197	0.0000 0.0031	R(30)	32516543.6413	0.0032 0.0049
R(32)	29477160.8619	0.0005 0.0031	R(32)	32550429.1766	0.0032 0.0049
R(34)	29511066.6779	0.0010 0.0033	R(34)	32583536.6462	0.0032 0.0049
R(36)	29544196.3278	0.0014 0.0034	R(36)	32615869.7050	0.0029 0.0047
R(38)	29576545.1272	0.0018 0.0036	R(38)	32647432.2414	0.0025 0.0045
R(40)	29608108.1438	0.0020 0.0037	R(40)	32678228.3735	0.0023 0.0044
R(42)	29638880.1916	0.0022 0.0038	R(42)	32708262.4434	0.0024 0.0044
R(44)	29668855.8268	0.0022 0.0038	R(44)	32737539.0114	0.0026 0.0045
R(46)	29698029.3424	0.0022 0.0038	R(46)	32766062.8511	0.0030 0.0048
R(48)	29726394.7624	0.0025 0.0040	R(48)	32793838.9430	0.0055 0.0066
R(50)	29753945.8365	0.0039 0.0050	R(50)	32820872.4688	0.0123 0.0128
R(52)	29780676.0338	0.0072 0.0079	R(52)	32847168.8049	0.0251 0.0254
R(54)	29806578.5363	0.0130 0.0134	R(54)	32872733.5159	0.0465 0.0466
R(56)	29831646.2326	0.0223 0.0225	R(56)	32897572.3487	0.0799 0.0800
R(58)	29855871.7107	0.0364 0.0366	R(58)	32921691.2249	0.1296 0.1296



Also, the error was reduced by about a factor of 10 as a result of this comparison. The previous interband difference measurement establishes  $R_{II}(10)$  as the absolute reference in the 9.4- $\mu\text{m}$  band without appreciable increase in error. To show how these calculated line frequencies differ from those of our previous experiment, we have plotted in Fig. 2 the differences for both the 9.4- and 10.4- $\mu\text{m}$  bands on a frequency scale relative to the band center. A striking feature in both of these plots is the approximately 10 kHz average shift in the  $P$  branch of both bands. The possibility of this shift was first pointed out by Clairon (21) and probably arose in the earlier experiment because neither measurements across the band centers nor low- $J$  ( $<10$ ) line frequency differences were measured. Another striking feature in the plot is the rapid departure at high- $J$  values of the measured line frequencies from the values predicted by constants obtained from low- $J$  frequency measurements. At the highest- $J$  values, the measured frequencies differed from the values predicted by the old constants by two to three times the estimated standard errors. Because the new analysis has similar problems, related in part to truncation of the power series expansion and imprecision in the experimental data, the statistically estimated uncertainties in Table V may tend to be underestimated, particularly outside the ranges  $P_I(50)$  to  $R_I(48)$  and  $P_{II}(48)$  to  $R_{II}(42)$ .

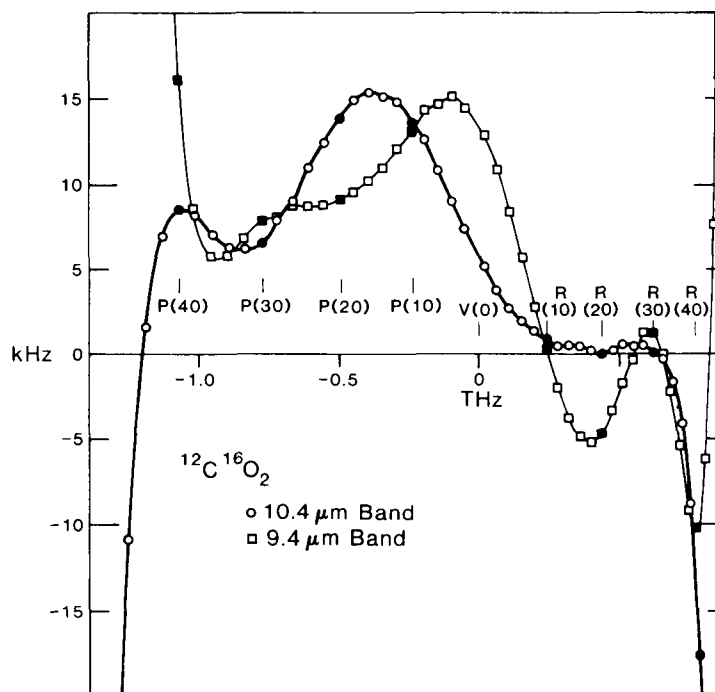


FIG. 2. Line frequencies for  $^{12}\text{C}^{16}\text{O}_2$  calculated with constants given in this paper minus frequencies calculated with constants from our previous measurement (11). Note the approximately 10-kHz average frequency shift in the  $P$ -branch of both bands and the rapid increase in the difference for high- $J$  values, i.e., for  $J$  values greater than the range of measurements in the previous experiment. In this plot, the old line frequencies were increased by 4.7 kHz to reflect the redetermination of the  $R_I(30)$  reference with respect to the methane frequency.

Measurement of  $P_I(50)$  in  $^{13}\text{C}^{16}\text{O}_2$  and  $R_{II}(26)$  in  $^{13}\text{C}^{18}\text{O}_2$ 

The line frequencies involved in the two different synthesis schemes represented by Eqs. (1) and (2) were determined by adding the appropriate measured frequency intervals relative to the 3.39- $\mu\text{m}$  methane line. Then, from Eqs. (1) and (2) and the measured difference frequencies in Table II, we obtained for  $P_I(50)$  the frequencies 26 035 339.9773 and 26 035 339.9776 MHz, respectively. For the final value, we took the average of these two measurements to give  $P_I(50)$ ,  $^{13}\text{C}^{16}\text{O}_2 = 26\ 035\ 339.9775(56)$  MHz. If we take the frequencies of the  $^{12}\text{C}^{16}\text{O}_2$  lines involved in the synthesis scheme from Table V, we obtain 26 035 339.9791 and 26 035 339.9746 MHz, respectively. The average, 26 035 339.9769 (63) MHz, is remarkably close to the previous result, and values from all four methods are extremely consistent. These results are summarized in Table VI.

Appropriate measured frequency intervals relative to the 3.39- $\mu\text{m}$  methane line were added to obtain the frequency of  $R_{II}(26)$  in  $^{13}\text{C}^{18}\text{O}_2$ . The result, 31 287 036.4117(48) MHz, is nearly the same as the value 31 287 036.4130(45) MHz obtained by using the tabulated value for  $P_{II}(10)$  and the measured  $P_{II}(10)-R_{II}(26)$ ,  $^{13}\text{C}^{18}\text{O}_2$  difference. The results are summarized in Table VI.

The frequencies measured here for  $P_{II}(28)$  and  $P_I(50)$  in  $^{13}\text{C}^{16}\text{O}_2$  and  $R_{II}(26)$  in  $^{13}\text{C}^{18}\text{O}_2$  are consistent with the values obtained by Freed *et al.* (9) but with over an order of magnitude reduction in error. The result for  $P_{II}(28)$  appears to agree with that of Clairon *et al.* (13) within the error limits.

TABLE VI  
Measurement of  $P_I(50)$ ,  $^{13}\text{C}^{16}\text{O}_2$  and  $R_{II}(26)$ ,  $^{13}\text{C}^{18}\text{O}_2$

$P_I(50), ^{13}\text{C}^{16}\text{O}_2$		
Synthesis	Determination of Synthesis Lines	
	From Meas. Int.	Table
$[2R_I(12)-R_{II}(10)]$	26 035 339.9773(68)	26 035 339.9791(67)
$[2P_I(34)-P_{II}(28), ^{13}\text{C}^{16}\text{O}_2]$	26 035 339.9776(90)	26 035 339.9746(106)
Average, $P_I(50), ^{13}\text{C}^{16}\text{O}_2$	26 035 339.9775(56) <sup>a</sup>	26 035 339.9769(63)
$R_{II}(26), ^{13}\text{C}^{18}\text{O}_2$		
Synthesis	Determination of $P_{II}(10)$	
	From Meas. Int.	Table
$P_{II}(10)$	31 287 036.4117(48) <sup>a</sup>	31 287 036.4130(45)

(a) Value used in the visible frequency measurements (7,8).

## DISCUSSION

In summary, with a few large interval frequency measurements between lines in the normal laser bands, we have been able to make significant improvements in the rovibrational constants of  $^{12}\text{C}^{16}\text{O}_2$ . In addition, a new measurement relative to the 3.39- $\mu\text{m}$  methane reference has reduced the absolute error of the  $\text{CO}_2$  reference line in each band. The total effect is that the frequencies of the Doppler-free stabilized laser lines in the 9.4- and 10.4- $\mu\text{m}$  bands are now known to better than two parts in  $10^{10}$ . Significant improvements in these accuracies will require improvements in the reproducibilities of the lasers themselves, as well as a better absolute reference frequency. Recent success with a high mixing order, two-step chain from  $P_1(50)$  in  $^{13}\text{C}^{16}\text{O}_2$  to the primary Cs frequency standard with Schottky and MIM diodes for harmonic generation and mixing makes progress in this direction quite plausible.

RECEIVED: July 11, 1983

## REFERENCES

1. See, e.g., F. R. PETERSEN, K. M. EVENSON, D. A. JENNINGS, AND A. SCALABRIN, *IEEE J. Quantum Electron.* **QE-16**, 319–323 (1980).
2. C. R. POLLOCK, F. R. PETERSEN, D. A. JENNINGS, J. S. WELLS, AND A. G. MAKI, *J. Mol. Spectrosc.* **99**, 357–368 (1983).
3. H. KILDAL, R. S. ENG, AND A. H. M. ROSS, *J. Mol. Spectrosc.* **53**, 479–488 (1974).
4. D. A. JENNINGS, F. R. PETERSEN, AND K. M. EVENSON, *Appl. Phys. Lett.* **26**, 510–511 (1975).
5. K. M. EVENSON, J. S. WELLS, F. R. PETERSEN, B. L. DANIELSON, AND G. W. DAY, *Appl. Phys. Lett.* **22**, 192–195 (1973).
6. D. A. JENNINGS, F. R. PETERSEN, AND K. M. EVENSON, *Opt. Lett.* **4**, 129–130 (1979).
7. C. R. POLLOCK, D. A. JENNINGS, F. R. PETERSEN, J. S. WELLS, R. E. DRULLINGER, E. C. BEATY, AND K. M. EVENSON, *Opt. Lett.* **8**, 133–135 (1983).
8. D. A. JENNINGS, C. R. POLLOCK, F. R. PETERSEN, R. E. DRULLINGER, K. M. EVENSON, J. S. WELLS, J. L. HALL, AND H. P. LAYER, *Opt. Lett.* **8**, 136–138 (1983).
9. C. FREED, L. C. BRADLEY, AND R. G. O'DONNELL, *IEEE J. Quantum Electron.* **QE-16**, 1195–1206 (1980).
10. F. R. PETERSEN, D. G. McDONALD, J. D. CUPP, AND B. L. DANIELSON, *Phys. Rev. Lett.* **31**, 573–576 (1973).
11. F. R. PETERSEN, D. G. McDONALD, J. D. CUPP, AND B. L. DANIELSON, "Laser Spectroscopy" (R. G. Brewer and A. Mooradian, Eds.), pp. 555–569, Plenum, New York, 1973.
12. D. J. E. KNIGHT, G. J. EDWARDS, P. R. PEARCE, AND N. R. CROSS, *IEEE Trans. Instrum. Meas.* **IM-29**, 257–264 (1980).
13. A. CLAIRON, B. DAHMANI, J. RUTMAN, *IEEE Trans. Instrum. Meas.* **IM-29**, 268–272 (1980); Laboratoire Primaire du Temps et des Fréquences, Paris, Rapport d'Activité, 1981, pp 24–31 (unpublished).
14. Y. S. DOMNIN, N. B. KOSHELJAEVSKY, V. M. TATARENKOV, AND P. S. SKUNJATSKY, *JETP Lett.* **34**, 167–170 (1981).
15. V. P. CHEBOTAYEV, *J. Phys. (Paris)* **42**, C8-505–C8-512 (1981).
16. C. FREED AND A. JAVAN, *Appl. Phys. Lett.* **17**, 53–56 (1970).
17. CH. BORDÉ AND J. L. HALL, "Laser Spectroscopy" (R. G. Brewer and A. Mooradian, Eds.), pp. 125–142, Plenum, New York, 1973.
18. J. L. HALL, private communication.
19. For methane stabilized laser intercomparisons, see, e.g., B. W. JOLLIFFE, G. KRAMER, AND J.-M. CHARTIER, *IEEE Trans. Instrum. Meas.* **IM-25**, 447–450 (1976) and J.-M. CHARTIER, *IEEE Trans. Instrum. Meas.* **IM-32**, 81–83 (1983).
20. D. HOGBEN, S. T. PEAVY, AND R. N. VARNER, "Omnitab II User's Reference Manual," NBS Technical Note 552, Superintendent of Documents, U. S. Govt. Printing Office, Washington, D. C.
21. A. CLAIRON, A. VAN LERBERGHE, C. SALOMON, M. OUHAYOUN, AND C. J. BORDÉ, *Opt. Commun.* **35**, 368–372 (1980).